SHOCK-INDUCED DECARBONATION IN AN OPEN SYSTEM USING A 2-STAGE LIGHT GAS GUN.
K. Kurosawa[1], S. Ohno[2], S. Sugita[3], T. Mieno[4], and S. Hasegawa[1], [1]ISAS/JAXA (3-1-1, Chuo-ku, Yoshinodai, Kanagawa 252-0222, Japan; kurosawa.kosuke@jaxa.jp), [2]PERC, Chiba Inst. of Tech., [3]Graduate school of Frontier Sci., The Univ. of Tokyo, [4]Dept. of Phys. Shizuoka Univ.

Introduction: Impact-induced vaporization/devolatilization processes may have played an important role in the origin of atmosphere [e.g., 1], ocean [2], and life [3] and intense global environmental perturbation during Earth's history [e.g., 4-6].

The shock-induced devolatilization of carbonates has been widely investigated in a number of previous studies [e.g., 4, 7, 8]. The amount of degassed CO_2, however, is still controversial because the peak shock pressure for incipient devolatilization for calcite (hereafter, referred as "decarbonation pressure") has large uncertainty. After shockwave passage due to a hypervelocity impact, a shock-compressed carbonate expands into an ambient space along an isentrope. If the peak shock pressure is larger than the decarbonation pressure, the shocked carbonate reaches the decarbonation boundary on a *P-T* diagram resulting from the isentropic release [e.g., 9], i.e., decarbonation occurs. ANEOS calculation predicts the decarbonation pressure to be 55 GPa [4]. In contrast, previous impact experiments detected shock-induced CO_2 gas at the peak shock pressures from 18-25 GPa [7, 8]. A series of decarbonation experiments in an open system at a wide range of peak shock pressures are necessary to resolve this discrepancy because serious problems were pointed out for using stainless containers [e.g., 9]. In this study, we developed an experimental method for shock-induced devolatilization in an open system using a two-stage light gas gun to investigate the decarbonation pressure of calcite.

Experiments: We conducted impact decarbonation experiments in an open system using a quadrapole mass spectrometer (QMS) and a two-stage light gas gun at Institute of Space and Astronautical Science (ISAS/JAXA). We added 3 new components in front of an experimental chamber (~40 L), a chamber with large volume (~2000 L) for gas dissipation (hereafter referred as "dissipation chamber"), a plastic diaphragm with the thickness of 12 μm, and an automatic gate valve, to minimize the chemical contamination from the acceleration gas by the gun. Figure 1 shows a schematic diagram of the experimental system. At this facility, the pressure in the dissipation chamber after a shot was ~700 Pa. Thus, the intrusion of the acceleration gas from the gun into the experimental chamber does not occur if the chamber is filled with chemically inert gas with the pressure much higher than 700 Pa. The plastic diaphragm was used to keep the inert gas in the chamber before the shot. The accelerated projectile easily penetrates the plastic diaphragm and impacts onto a calcite target. The automatic gate valve was used to prevent the dissipation of impact-induced gases from the hole on the diaphragm produced by the projectile to the outside of the experimental chamber. This valve was operated at ~0.1 s after the impact using the electric signal at the shot.

We used an Al_2O_3 sphere with diameter of 3.2 mm and a natural calcite block with size of 10 x 10 x 10 cm as projectile and target, respectively. A basalt block was also used for blank experiment. Impact velocity was varied from 1.9 km/s and 6.7 km/s. This range of the velocity corresponds to 20 – 110 GPa. Impact angle was fixed at 90° from the horizontal (i.e., vertical impact only). An argon gas was used for the chemically inert gas. We produced the gas flow of Ar in the chamber to introduce the shock-induced gases from the experimental chamber to the QMS efficiently (i.e., flow system). The equilibrium pressure in the experimental chamber was fixed at 2700 Pa, which was ~4 times the pressure of the contaminant gas in the dissipation chamber after the shot. The pressure in the QMS was fixed at 2 x 10^{-3} Pa. Calibration experiments were also conducted with Ar-CO_2 gas mixtures with a variety of CO_2 mixing ratio.

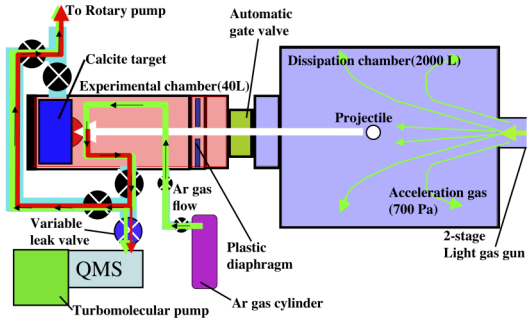

Fig. 1. A schematic diagram of the experimental system.

Experimental results: We used H_2, M/Z=2, as the indicator of the contaminant gas because H_2 is the main component of the contaminant gas (>99%) under our experimental condition. Figure 2a shows the time series data of the ion current for H_2. The changes in the ion current of H_2 after the impact were not observed excepted for #1312. In addition, the increase in the ion current of H_2 for #1312 was only ~10% relative to the base level, suggesting that we could mostly avoid the

chemical contamination from the acceleration gas of the gun. Figure 2b shows the time series data of the ion current for M/Z=36, which corresponds to Ar. The ion currents for Ar were very stable even when the impact occurred in the chamber. In contrast, the ion currents for CO_2, M/Z=44, drastically increased after the impacts as shown in Figure 3a. Note that the peak values of the CO_2 ion current with calcite targets are ~10 times that with basalt targets as blank experiments at the same impact velocity. Thus, the most part of detected CO_2 was produced from the calcite due to shock heating. To estimate the CO_2 amount at the impact, we fitted the decay curve of the CO_2 ion current with exponential function, $A\exp(-t/B)$ where *A, t,* and *B* are the CO_2 ion current at the time origin, the time after the impact, and the characteristic time for decay, respectively. The uncertainties in this estimation was ~10%. We calculated the absolute impact-induced CO_2 amount based on the current ratio of CO_2 to Ar at the time origin. Figure 3b shows the amount of impact-induced CO_2 as a function of peak shock pressure calculated based on the 1-D impedance matching method [10] and the linear velocity relation for calcite [10] and for Al_2O_3 [11]. The shock-induced CO_2 was detected at 20 GPa. This is consistent with the previous experiments [7, 8]. The produced CO_2 amount strongly depends on impact velocity. The CO_2 amount at 6.7 km/s was ~500 times that at 1.9 km/s. We found that the peak shock pressure dependence on the CO_2 amount changes around 60 GPa, which corresponds to the decarbonation pressure predicted by ANEOS (55GPa, [4]). If we fitted the CO_2 amount using a linear function of peak shock pressure, the slope at >60 GPa is 4.2 times than that at <60 GPa.

Discussion & Conclusions: Here, we discuss the origin of the change in the slope around 60 GPa. *Kondo & Ahrens* [12] measured peak shock temperature of calcite at 40 GPa, showing that the peak shock temperature at 40 GPa is ~2000 K higher than a prediction based on thermodynamical calculation. In contrast, the measured peak shock temperature of calcite at 95 GPa is consistent with the theory [13]. This difference is caused by heterogeneous heating due to shear banding at low peak shock pressure [12]. Thus, observed shock-induced decarbonation with low efficiency at <60 GPa is expected to be caused by such local energy concentration. The equilibrium shock heating in the target may occur at >60 GPa and is expected to lead to massive decarbonation. Hense, "the effective decarbonation pressure of calcite" is close to the ANEOS prediction. Although the shock-induced decarbonation of calcite occurs at 20 GPa, its efficiency is very low because it is occurred locally.

In this study, we present a new experimental method for gas-phase chemical analysis in an open system using a two-stage light gas gun and the results of shock decarbonation experiments with a wide range of peak shock pressures. Our system can be directly applied to the quantitative measurements including chemical composition of impact-induced gases using other solid materials. The system may serve as a powerful tool for understanding of the nature of shock-induced vaporization/devolatilization and post-impact chemistry.

References: [1] Hashimoto et al. (2007), *JGR*, **112**, E05010, doi:10.1029/2006JE002844. [2] Matsui and Abe (1986), *Nature,* **319**, 303. [3] Mukhin et al. (1989), *Nature,* **340**, 46. [4] Pierazzo et al. (1998), *JGR*, **103**, 28607. [5] Ohno et al. (2004), *EPSL*, **218**, 347. [6] Kawaragi et al. (2009), *EPSL*, **282**, 56. [7] Boslough et al. (1982), *EPSL*, **61**, 166. [8] Ohno et al. (2008), *GRL*, **35**, L13202, doi:10.1029/2008GL033796. [9] Ivanov and Deutsch (2002), *Phys. Earth and Planet. Int.*, **129**, 131. [10] Melosh (1989), *Impact cratering A geologic processes*, Oxford University Press, New York, 1989. [11] Marsh (1980), *LASL Shock Hugoniot Data*, Univ. California Press, Berkeley, California. [12] Kondo and Ahrens (1983), *Phys. and Chem. of Minerals*, **9**, 173. [13] Gupta et al. (2002), *EPSL*, **201**, 1.

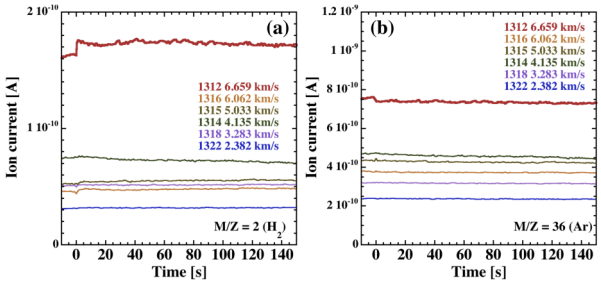

Fig. 2. Time series data of ion current for H_2 (a) and for Ar (b) after the impact. Impact velocities are indicated in the figure.

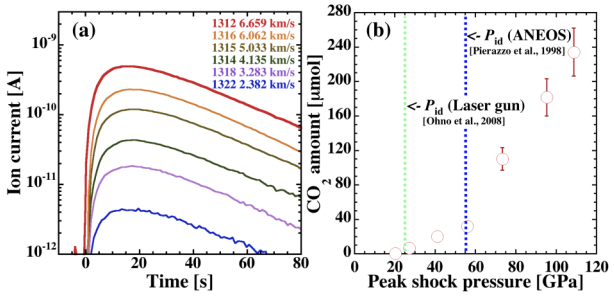

Fig. 3. Time series data of ion current for impact-induced CO_2 (a), and the CO_2 amount as a function of peak shock pressure (b). P_{id} in panel (b) means the pressure for incipient decarbonation.